Hindawi
Advances in Civil Engineering
Volume 2023, Article ID 4675152, 9 pages
https://doi.org/10.1155/2023/4675152

Research Article

Research on Upper Bound Limit Stability Analysis of Multi-Step High Steep Slope

Zhen Wang

School of Engineering, Huanghe Science and Technology College, Zhengzhou, Henan, China

Correspondence should be addressed to Zhen Wang; hhstu_wz@163.com

Received 27 March 2023; Revised 17 April 2023; Accepted 29 April 2023; Published 15 May 2023

Academic Editor: Paolo Castaldo

In order to explore the stability of multi-step high steep slope, this paper considers layer distribution of soil and builds a slope failure mechanism which meets requirements of velocity separation based on plastic mechanics principles, then derives the calculation method of external force power and internal energy dissipation power in failure area using numerical analysis theory, and proposes a loop algorithm for slope stability analysis combining upper bound limit analysis theorem and strength reduction principle. At the same time, in order to enhance the applicability of the upper bound limit analysis method, this paper develops a slope stability calculation system of upper bound limit analysis combined with computer programming technology and evaluates the accuracy of the calculation system through slope engineering practice in open-pit mine. The results show that stability factor by calculation system of upper bound limit analysis is an upper limit solution compared with limit equilibrium method, but the error rate of two methods is less than 5%, which indicates that the slope stability calculation system established in this paper has high accuracy in stability analysis of multi-step high steep slope in the practice of open-pit mine. On the other hand, the most dangerous sliding surface searched by upper bound limit analysis can fully solve velocity problems of multi-step high steep slope failure, so it has stronger reference values in engineering practice.

1. Introduction

In recent years, with the vigorous development of civil engineering construction, multi-step high steep slopes are becoming more common in highways, water conservancies, mines, constructions, and other fields [1–3]. This kind of slope is characterized by wide distribution, poor stability, and difficult landslide management, and its stability has become an important issue to be urgently solved in slope practice [4, 5].

The common methods of slope stability analysis mainly include the limit equilibrium method and limit analysis method [6, 7]. In the 1920s, Fellenius proposed the Swedish circular arc method, which has established the beginning of the limit equilibrium method [8–10]. In the following decades, the simplified Bishop method, Morgenstern–Price method, Sarma method, simplified Janbu method, residual thrust method, and other limit equilibrium methods were successively proposed [11–16]. Over nearly a century's development, the limit equilibrium method has developed from a simplified empirical algorithm to a mature method with complete theoretical systems, which is widely used in slope engineering practice [17]. These abovementioned methods only met parts of static equilibrium conditions and moment equilibrium conditions, but the relationship between stress and strain of soil was not considered effectively. A series of assumptions must be introduced to make the problem solvable, and these assumptions will lead to errors in the calculation [18, 19]. The limit analysis method based on plastic principles has gradually become a research hotspot in slope engineering practice in order to overcome deficiencies of the limit equilibrium method. Furthermore, upper bound limit analysis seeks the slope failure mechanism by establishing movement permissible velocity field, which has a strict theoretical foundation and a rigorous derivation process and can fully solve the velocity problems of slope failure [20–22]. In the 1970s, Chen led upper bound limit analysis into geotechnical engineering practices and proposed upper bound limit analysis for slope stability calculation [23]. In the 1990s, Michalowski divided sliding body within slope failure areas vertically and put forward upper bound limit analysis for translational failure forms [24]. On this basis, Donald divided sliding body within slope failure areas slantwise and put forward upper bound limit analysis for combined translational failure forms and inclined failure forms [25].

Obviously, upper bound limit analysis has its unique advantages in slope stability analysis [26]. It provides a good solution to the problem of homogeneous slope stability [27], but the applicability of upper bound limit analysis is greatly limited for complex terrain conditions due to the limitation of solving process [28, 29]. Aiming at this problem, on the basis of considering the layered distribution of soil, this paper researches on the stability of multi-step high steep slope in engineering practice, proposes upper bound limit analysis algorithm of multi-step high steep slope stability, and develops a widely applicable analysis system based on computer programming technology. The results will enhance the applicability of the upper bound limit analysis method in slope engineering practice, which has important significance and popularization values.

2. Stability Analysis of Multi-Step High Steep Slope

2.1. Slope Morphology and Soil Parameters. For the high steep slope composed by n steps, the morphological parameters of each step are defined as follows. Height of each step is $h_1, h_2, \ldots, h_n$, slope angle of each step is $\alpha_1, \alpha_2, \ldots, \alpha_n$, and plate width of each step is $b_1, b_2, \ldots, b_{n-1}$. At the same time, considering the layered distribution characteristics of slope soil in engineering practice, the slope consists of m layers soil, and the mechanical parameters of soil in each layer are defined as follows from top to bottom. Thickness of each soil layer is $h_1', h_2', \ldots, h_m'$, density of each soil layer is $\gamma_1, \gamma_2, \ldots, \gamma_m$, cohesion of each soil layer is $c_1, c_2, \ldots, c_m$, and internal friction angle of each soil layer is $\varphi_1, \varphi_2, \ldots, \varphi_m$. The slope morphology and soil parameters are shown in Figure 1.

Obviously, for the high steep slope consisting of n steps, when the morphological parameters of each step are known, the slope height and the slope angle can be calculated through plane geometric relationship, and the slope morphology can be uniquely obtained.

2.2. Calculation Model Establishment of High Steep Slope

2.2.1. Mathematical Model Establishment of Failure Mechanism. The plastic theory shows that when shear failure occurs, the slip surface morphology is logarithmic spiral [30, 31]. For the high steep slope in Figure 1, shear failure may occur at toe point of each step $A_1, A_2, \ldots, A_n$. This paper assumes that shear failure occurs at the point of A_n to illustrate the calculation process, and shear failure occurs at other points which can be calculated in the same way. The failure mechanism is formed by intersecting parts of m logarithmic spirals when shear failure occurs at point of A_n. At the same time, the failure mechanism starts at the top point of slope B_0 and passes through the toe point of slope A_n. The failure mechanism is shown in Figure 2.

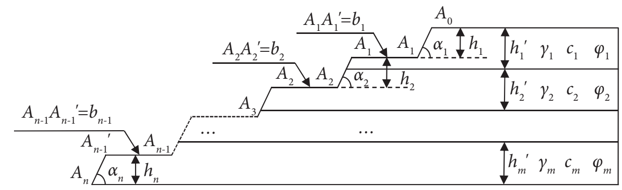

Figure 1: Slope morphology and soil parameters.

In Figure 2, r (m) is the line segment distance between the rotation center and the logarithmic spiral, and θ (rad) is the horizontal angle for the line between the rotation center and the logarithmic spiral. According to unique velocity of the slope failure mechanism at soil layer interface, it can be obtained that the combined logarithmic spiral has the same angular velocity ω and the same rotation center O, so the equation of the slope failure mechanism can be expressed as

$$r = a_i e^{\theta \tan\varphi_i}, \quad (i = 1, 2, 3 \ldots m). \tag{1}$$

Establish a searching area of rotation center above the shoulder point of the slope; for any point in the searching area, polar coordinate of the toe point A_n (r_m, θ_m) is definite. Then, for any definite r_m and θ_m, the parameter value a_m in the mth logarithmic spiral can be calculated. According to coordinate consistency of the failure mechanism at the soil layer interface, the parameters $a_{m\text{-}1}, a_{m-2}, \ldots, a_2, a_1$ can be calculated layer by layer from bottom to top. On this basis, the slope failure mechanism equation can be obtained. So, the slope failure mechanism equation can be uniquely controlled by the position of rotation center.

2.2.2. Mathematical Model Establishment of Slope Morphology. According to the above introductions, for any point in the searching area, polar coordinate of the toe point A_n (r_m, θ_m) is definite, so the plane rectangular coordinate of the toe point A_n can be expressed as $(r_m \cdot \cos\theta_m, -r_m \cdot \sin\theta_m)$. Therefore, slope equation of the n^{th} step can be expressed as formula (2) according to slope angle of the n^{th} step which is α_n.

$$x = g_n(y) = (y + r_m \cdot \sin\theta_m) \cdot \cot\alpha_n + r_m \cdot \cos\theta_m. \tag{2}$$

According to the step distribution morphology, the plane rectangular coordinate of the toe point of the n_1^{th} step A_{n-1} can be expressed as $(r_m \cdot \cos\theta_m + h_n \cdot \cot\alpha_n + b_{n\text{-}1}, -r_m \cdot \sin\theta_m + h_n)$. With the same reasoning as above, slope equation of the $(n\_1)^{\text{th}}$ step can be expressed as

$$\begin{aligned} x = g_{n-1}(y) &= (y + r_m \cdot \sin\theta_m - h_n) \cdot \cot\alpha_{n-1} \\ &\quad + r_m \cdot \cos\theta_m + h_n \cdot \cot\alpha_n + b_{n-1}. \end{aligned} \tag{3}$$

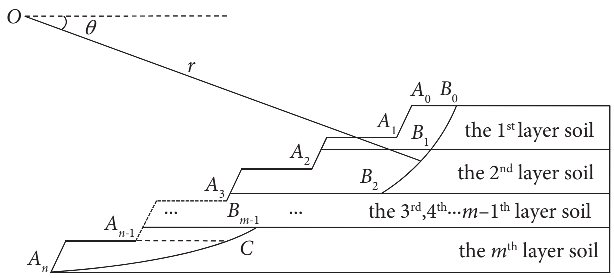

Figure 2: Failure mechanism schematic diagram of high steep slope.

In the same way, slope equation can be obtained according to the plane rectangular coordinate of toe point and slope angle of each step, so the slope morphology equation can be obtained only by the position of rotation center.

Meanwhile, when the polar coordinate of the toe point A_n is (r_m, θ_m), the floor equation of the m^{th} layer soil can be expressed as $y = \_r_m \cdot \sin\theta_m$. So, roof equation of the m^{th} layer soil can be expressed as formula (4) according to the m^{th} layer soil thickness which is h_m'.

$$y = -r_m \cdot \sin\theta_m + h_m'. \tag{4}$$

With the same reasoning, as above, according to the $(m\_1)^{\text{th}}$ layer, soil thickness is h_{m-1}, and roof equation of the $(m\_1)^{\text{th}}$ layer soil can be expressed as

$$y = -r_m \cdot \sin\theta_m + h_m' + h_{m-1}'. \tag{5}$$

Similarly, floor equation and roof equation can be obtained according to each layer soil thickness, so floor equation and roof equation of slope layer soil can be determined only by the position of rotation center.

To sum up, failure mechanism, slope morphology, floor equation, and roof equation can be determined only by the position of rotation center. Then, the mathematical model of failure mechanism and slope morphology can be established through the position of rotation center.

2.3. Upper Bound Limit Analysis for Slope Stability. The upper bound limit analysis method analyzes slope stability from the way of energy and velocity. The basic theory of this method is that for any slope failure mechanism, when external force power is equal to internal energy dissipation power, the unsafe upper bound of failure loading can be obtained, and then the slope stability can be analyzed. Therefore, this paper takes the position of rotation center as initial parameter and proposes calculation methods of external force power and internal energy dissipation power of the slope. Furthermore, the upper bound limit analysis method for slope stability can be established by changing the position of the rotation center.

2.3.1. Calculation Method of External Force Power. In natural state, external force power of the failure area is all provided by gravity power [32, 33]. For the failure mechanism shown in Figure 2, the step plates are lengthened in reverse and intersect the failure mechanism (assuming that thickness of the m^{th} soil layer is higher than height of the n^{th} step). In the vertical direction, the step plates and soil layer interfaces divide the slope failure area into several horizontal strips. For the lowest horizontal strip $A_nA_{n-1}C$, its failure region S in the planar rectangular coordinate system can be expressed as

$$\begin{cases} y_0 \le y \le y + h_n, \\ g_n(y) \le x \le f_n(y), \end{cases} \tag{6}$$

where y_0 is the ordinate of the toe point, which can be solved by the formula $y_0 = -r_m \cdot \sin\theta_m$, $g_n(y)$ is the slope equation of the n^{th} step, it is shown in formula (2), and $f_n(y)$ is the logarithmic spiral equation of the m^{th} soil layer. On the premise that the position of rotation center is known, $g_n(y)$ and $f_n(y)$ can be uniquely determined. Therefore, external force power E' of the lowest horizontal strip can be expressed as

$$E' = \int_S \gamma \cdot v \, \mathrm{d}S, \tag{7}$$

where E' (kW) is the external force power of the lowest horizontal strip in the slope failure area, S (m^2) is the failure region of the lowest horizontal strip, dS (m^2) is the arbitrary area element, γ ($\mathrm{kN/m}^3$) is the soil density of the area element, and v(m/s) is the vertical direction velocity of the area element. According to the plane geometry, vertical direction velocity of the area element can be expressed as

$$v = \omega \cdot r \cdot \cos\theta = \omega \cdot x. \tag{8}$$

Therefore, formula (7) can be converted into

$$\begin{aligned} E' &= \int_S \gamma_m \cdot v \, \mathrm{d}S \\ &= \omega \cdot \gamma_m \int_{y_0}^{y_0+h_n} \mathrm{d}y \int_{g_n(y)}^{f_n(y)} x \mathrm{d}x \\ &= \frac{1}{2}\omega \cdot \gamma_m \int_{y_0}^{y_0+h_n} \left[f_n^2(y) - g_n^2(y)\right] \mathrm{d}y \\ &= \frac{1}{2}\omega \cdot \gamma_m \left[\int_{y_0}^{y_0+h_n} f_n^2(y)\mathrm{d}y - \int_{y_0}^{y_0+h_n} g_n^2(y)\mathrm{d}y\right], \end{aligned} \tag{9}$$

where $g_n(y)$ is a linear function about y, so the definite integral of $g_n^2(y)$ can be solved. However, because the function expression of $f_n(y)$ cannot be determined, the definite integral of $f_n^2(y)$ cannot be solved directly. In this paper, the complex Simpson method is applied to approximate calculation. Divide the lowest horizontal strip into $2k$ equal parts along the vertical direction and extract the coordinates of each equal point, denoted as (x_1, y_1), (x_2, y_2), ..., (x_{2k-1}, y_{2k-1}). Then, the definite integral of $f_n^2(y)$ can be approximated as

$$\int_{y_0}^{y_0+h_n} f^2(y)\mathrm{d}y \approx \frac{h_n}{6k}\left[x_{A_n}^2 + 4\left(x_1^2 + x_3^2 + \cdots + x_{2k-1}^2\right) + 2\left(x_2^2 + x_4^2 + \cdots + x_{2k-2}^2\right) + x_C^2\right], \tag{10}$$

where x_{A_n} and x_C represent the corresponding abscissa of point A_n and point C, x_1, x_2, x_3, ..., x_{2k-1} represent the corresponding abscissa of the 1st, 2nd, 3rd... $2k_1$th equal points, and the abscissa of each equal point can be expressed as

$$\begin{cases} x_1 = f_n(y_1) = f_n\left(y_0 + \dfrac{h_n}{2k}\cdot 1\right), \\ x_2 = f_n(y_2) = f_n\left(y_0 + \dfrac{h_n}{2k}\cdot 2\right), \\ \cdots \\ x_{2k-1} = f_n(y_{2k-1}) = f_n\left[y_0 + \dfrac{h_n}{2k}\cdot(2k-1)\right]. \end{cases} \tag{11}$$

The abscissa of each equal point is known because the failure mechanism is unique, so the definite integral of $f_n^2(y)$ can be solved and external force power of the lowest horizontal strip in the failure region can be calculated. Similarly, external force power of each horizontal strip can be calculated from bottom to top, and external force power E of the failure area of high steep slope can be finally determined by adding external force power of each strip.

2.3.2. Calculation Method of Internal Energy Dissipation Power. Upper bound limit analysis assumes that the slope soil is rigid material and the velocity of soil inside and outside the slope slip surface is continuous. Obviously, the velocity discontinuity only occurs on the slip surface, the same with combined logarithmic spiral [34–36]. Therefore, internal energy dissipation power in failure area of high steep slope concentrates on intersecting parts of m logarithmic spirals. For the soil in the mth layer, $rd\theta\cdot(\cos\varphi_m)^{-1}$ on the logarithmic spiral is selected as element length, and the corresponding cohesion force of the element length can be expressed as $c_m rd\theta\cdot(\cos\varphi_m)^{-1}$, and then internal energy dissipation power of the mth soil layer can be expressed as

$$\begin{aligned} D_m &= \int_{\theta_{m-1}}^{\theta_m} v\cos\varphi_m\cdot c_m \mathrm{r}\mathrm{d}\theta\cdot(\cos\varphi_m)^{-1} \\ &= c_m\cdot\omega\int_{\theta_{m-1}}^{\theta_m} r^2\mathrm{d}\theta = \frac{c_m\cdot\omega}{2\tan\varphi_m}\left(r_m^2 - r_{m-1}^2\right), \end{aligned} \tag{12}$$

where D_m (kW) is the internal energy dissipation power of the mth soil layer in the slope, θ_{m-1} (rad) is the horizontal angle for the line between rotation center and starting point of failure mechanism in the mth soil layer, and r_{m-1} (m) is the length for the corresponding line. Obviously, on the premise that the position of rotation center is known, both r_{m-1} and θ_{m-1} can be obtained. Therefore, internal energy dissipation power of the mth soil layer in the slope can be solved according to formula (12). Similarly, internal energy dissipation power of each soil layer can be calculated from bottom to top, and internal energy dissipation power of the high steep slope D can be determined by adding internal energy dissipation power of each soil layer.

2.3.3. Strength Reduction Algorithm for Slope Stability. For any imaginary failure mechanism, when external force power is greater than internal energy dissipation power, the slope soil cannot bear the applied load value, and then the failure will occur. The upper bound limit analysis method assumes that when external force power is just equal to internal energy dissipation power, the slope is in a limit equilibrium state, and the slope stability analysis can be calculated according to this limit equilibrium state [37–39]. For the slope in nonlimiting equilibrium state, repeated strength reduction is required to gradually transition the slope to the limit equilibrium state. The reduction formula can be expressed as

$$\begin{cases} c' = \dfrac{c}{F}, \\ \tan\varphi' = \dfrac{\tan\varphi'}{F}, \end{cases} \tag{13}$$

where F is the strength reduction coefficient, c and φ are cohesion and internal friction angle of the slope soil before strength reduction, and c' and φ' are cohesion and internal friction angle of the slope soil after strength reduction. This paper applied computer programming technology to realize strength reduction calculation of slope stability.

2.3.4. Slope Stability Analysis System Development. The strength reduction principle shows that when the strength reduction coefficient F is equal to the stability factor Fs, it indicates that slope is in a limit equilibrium state, and external force power E is exactly equal to internal energy dissipation power D, which means $(E–D)_{\max} = 0$, so build the following function:

$$\Delta = (E - D)_{\max}. \tag{14}$$

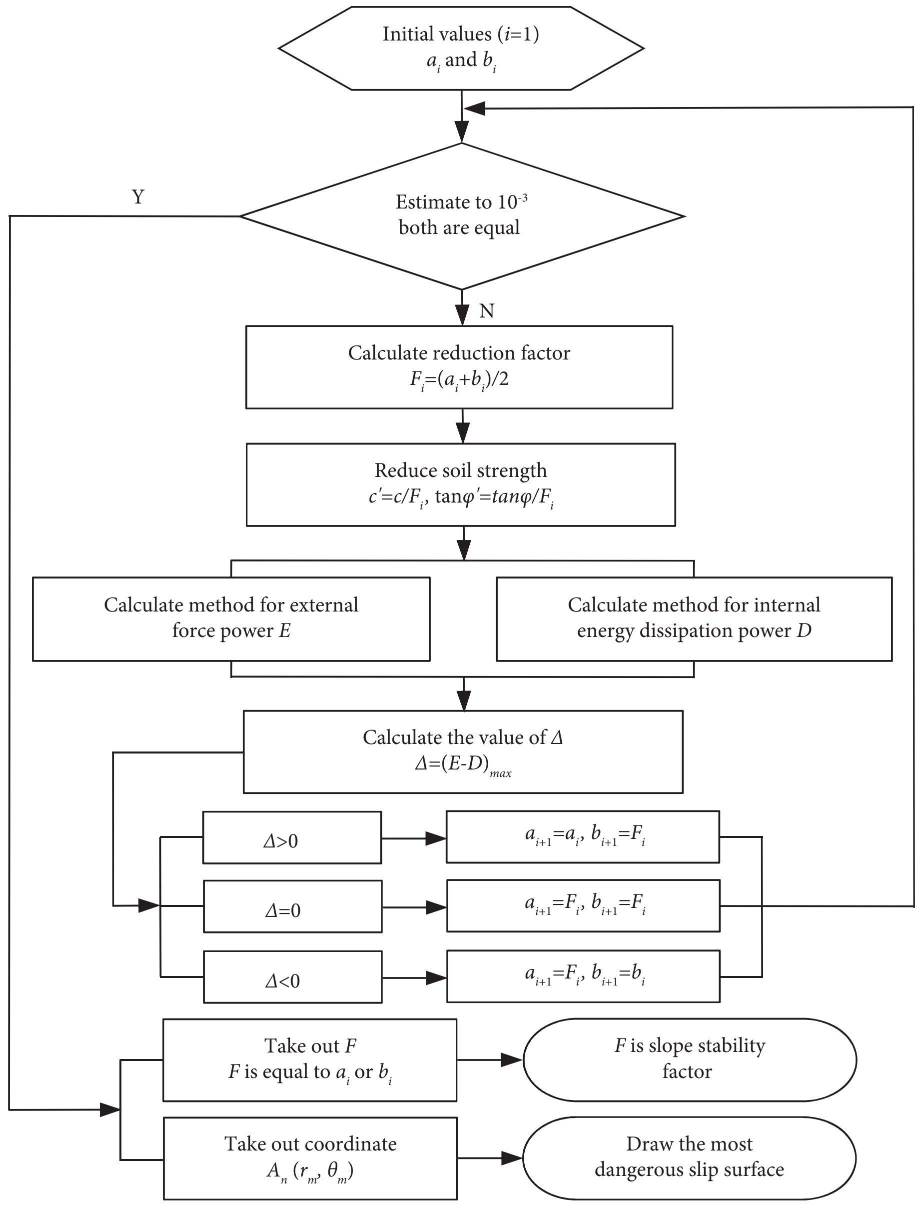

Figure 3: Calculation process of stability analysis system.

It is clear that Δ has only one zero point in the range of arithmetic numbers. Meanwhile, F and Δ are negatively correlated. According to the above two characteristics, a slope stability analysis system is developed by using the dichotomy method. The calculation process of slope stability analysis system is shown in Figure 3.

In Figure 3, the closed interval formed by a_i and b_i should strictly contain the slope stability factor at the condition that $i = 1$. Through Figure 3, the strength reduction coefficient F can be output, which is the slope stability factor Fs. Furthermore, the stability factor is accurately 10^{-3} and can fully meet the requirement of engineering practice. At the same time, the polar coordinate of the toe point can be output through Figure 3, and the slope slip surface can be drawn according to the toe point, which is the most dangerous slip surface of the slope.

3. Engineering Case Analysis

Due to requirements of mining and transportation, open-pit mine slope is usually designed in the form of multi-stage steps. In this paper, the complex slope in open-pit mine composed of dump slope and mining slope is selected as engineering background, and the accuracy of the stability analysis system is evaluated.

3.1. Slope Geology. The complex slope is composed of dump slope and mining slope. Dump slope is composed of two dump steps, height of each step is 24 m, slope angle of each step is 35°, and plate width of each step is 50 m. Mining slope is composed of six mining steps, height of each step is 12 m, slope angle of each step is 65°, and plate width of each step is 35 m. The distance between dump slope and mining slope is

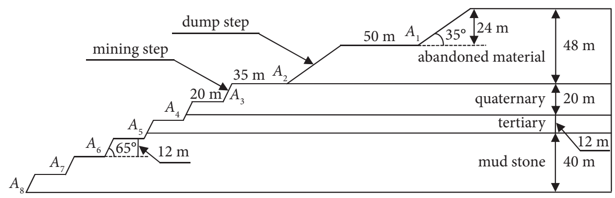

Figure 4: Slope morphology.

Table 1: Mechanical parameters of slope soil.

Soil layer	Height (m)	Density (kN·m^{-3})	Cohesion (kPa)	Internal friction angle (°)
Abandoned material	48	21	35	16
Quaternary	20	20.5	10	24
Tertiary	12	18.5	50	19
Mud stone	40	22.2	65	20.5

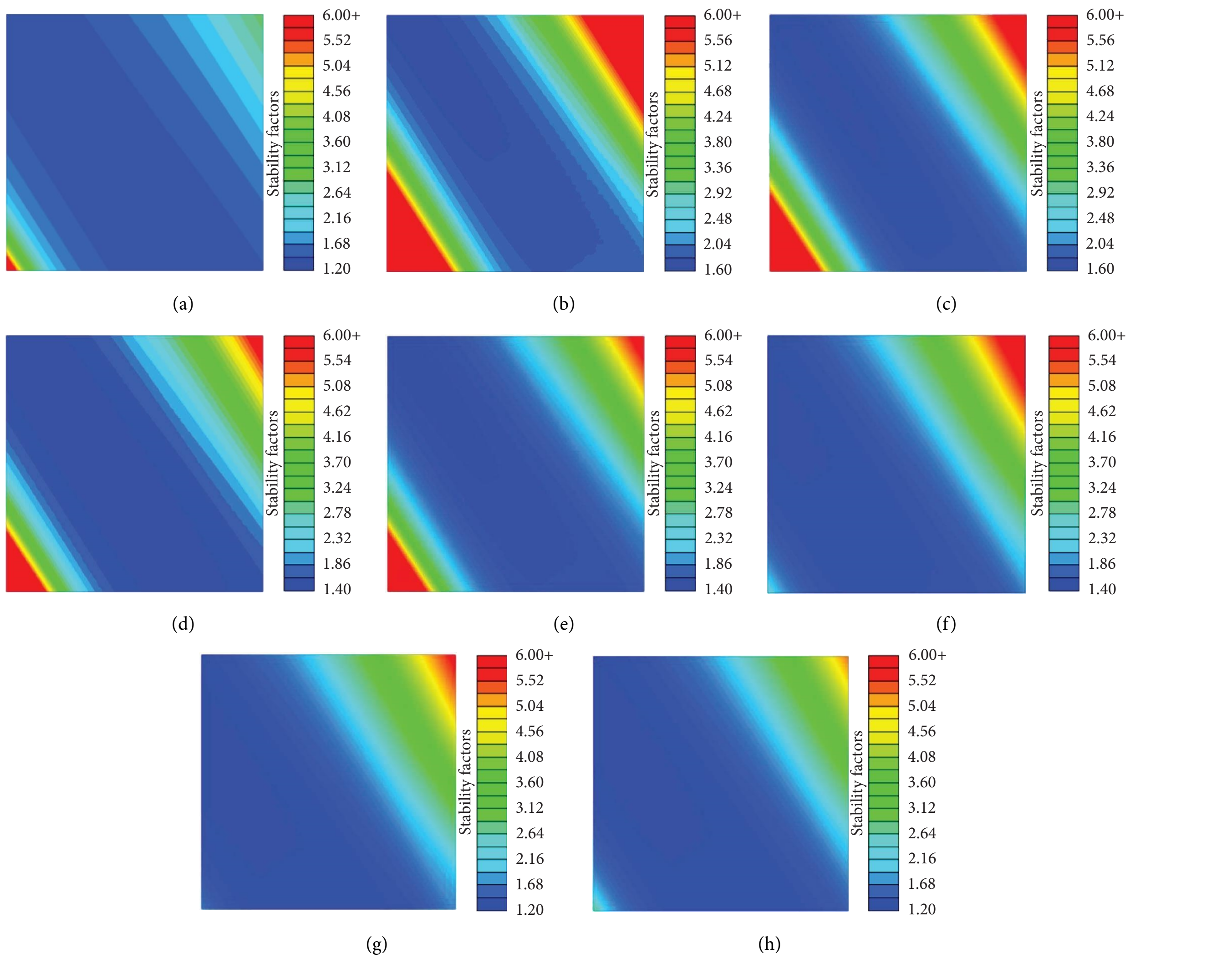

Figure 5: Stability factor distribution in the searching area. (a) Toe point is A_1 (Fs = 1.364). (b) Toe point is A_2 (Fs = 1.713). (c) Toe point is A_3 (Fs = 1.631). (d) Toe point is A_4 (Fs = 1.523). (e) Toe point is A_5 (Fs = 1.478). (f) Toe point is A_6 (Fs = 1.425). (g) Toe point is A_7 (Fs = 1.342). (h) Toe point is A_8 (Fs = 1.294).

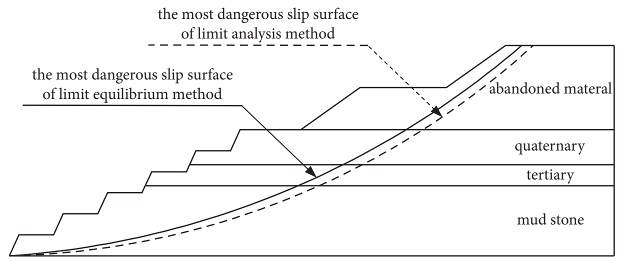

Figure 6: The most dangerous slip surface.

Table 2: Slope stability analysis results.

Slope toe point	Calculation method		Error rate (%)
	Limit analysis method	Limit equilibrium method	
A_1	1.364	1.321	3.26
A_2	1.713	1.655	3.50
A_3	1.632	1.574	3.68
A_4	1.524	1.472	3.53
A_5	1.478	1.426	3.65
A_6	1.425	1.371	3.94
A_7	1.342	1.296	3.55
A_8	1.294	1.246	3.85

35 m, and soil layer of the complex slope is composed of abandoned material, quaternary, tertiary, and mud stone from top to bottom. The slope morphology is shown in Figure 4, and the mechanical parameters of the slope soil are shown in Table 1.

3.2. Stability Analysis Results. Apply the analysis system described above to analyze and evaluate the slope stability. At the same time, in order to ensure stability of the slope, toe points of all steps $A_1, A_2, \ldots, A_8$ are selected as the slope toe point, and analyze the slope stability of the above eight conditions. The stability factor distribution in the searching area is shown in Figure 5.

It can be seen from Figure 5 that when A_8 is selected as slope toe point, the corresponding stability factor Fs = 1.294, and the stability factor reaches the minimum value, so the slope stability factor is 1.294. At the same time, the most dangerous sliding surface of the slope can be drawn according to the polar coordinates of the toe point, and the most dangerous sliding surface is shown in Figure 6.

3.3. Calculation Result Evaluation. The limit analysis method and limit equilibrium method analyze slope stability from different directions, but their calculation results should be highly consistent [40, 41]. This paper selects simplified Bishop method in the limit equilibrium method to evaluate accuracy of calculation results. The slope stability analysis results are shown in Table 2, and the most dangerous sliding surface is shown in Figure 6.

From the perspective of slope stability factor, the error rate of calculation results of two methods is less than 5%, which can fully meet the requirements of slope practice. It indicates that the slope stability calculation system established in this paper has high accuracy in stability analysis of multi-step high steep slopes in the practice of open-pit mines.

On the other hand, from the perspective of the most dangerous sliding surface, the position of starting point and ending point of landslide in the calculation results of two methods is approximately the same. But the most dangerous sliding surface searched by upper bound limit analysis can fully solve velocity problems of multi-step high steep slope failure [42], so it has stronger reference values in engineering practices.

4. Conclusion

This paper proposes a calculation method of upper bound limit analysis for multi-step high steep slope stability, develops a cycle program of stability analysis system, and then evaluates the accuracy of analysis system through engineering practice. The main conclusions are as follows:

(1) The layered distribution law of slope soil in engineering practice is analyzed, and according to the basic principle of plastic mechanics, the failure mechanism of multi-step high steep slope which can meet the requirement of velocity separation is constructed.

(2) The calculation method of external force power and internal energy dissipation power in the failure area is derived, and combined with upper bound limit analysis theorem and strength reduction principle, upper bound limit analysis cycle algorithm suitable for the stability of multi-step high steep slope is proposed.

(3) The slope stability analysis system is developed, and the accuracy of the analysis system is evaluated according to the engineering practice, which fully

verifies the applicability of the analysis system in slope engineering practice.

Data Availability

The data used to support the findings of this study are available from the corresponding author upon request.

Conflicts of Interest

The author declares that there are no conflicts of interest regarding the publication of this paper.

Acknowledgments

This study was supported by the Key Research Project for Higher Education in Henan Province (22B560005) and the Scientific and Technological Project in Henan Province (202102310567).

References

[1] S. Suman, S. Z. Khan, S. K. Das, and S. K. Chand, "Slope stability analysis using artificial intelligence techniques," *Natural Hazards*, vol. 84, no. 2, pp. 727–748, 2016.
[2] Z. Wang, "Research on landslide warning model establishment and disaster space-time evolution analysis," *Advances in Civil Engineering*, vol. 2021, Article ID 7496940, 10 pages, 2021.
[3] B. He, H. Tao, A. Wei, S. Liu, and H. Li, "Model test of influence of slope surface morphology on dynamic deformation failure," *Rock and Soil Mechanics*, vol. 30, no. 2, pp. 111–117, 2014.
[4] N. Vatanpour, M. Ghafoori, and H. H. Talouki, "Probabilistic and sensitivity analyses of effective geotechnical parameters on rock slope stability: a case study of an urban area in northeast Iran," *Natural Hazards*, vol. 71, no. 3, pp. 1659–1678, 2014.
[5] D. Liu, J. Gao, F. Chen, S. Hu, X. Zhao, and Y. Li, "Analysis of mechanical properties and slope stability of red bed soft rock: a case study in Xinjiang irrigation diversion channel," *Advances in Civil Engineering*, vol. 2022, Article ID 9453702, 9 pages, 2022.
[6] D. P. Deng and L. Li, "Research on calculation methods of slope stability under two types of sliding surface," *Rock and Soil Mechanics*, vol. 34, no. 2, pp. 372–410, 2013.
[7] X. P. Zhou and H. Cheng, "Analysis of stability of threedimensional slopes using the rigorous limit equilibrium method," *Engineering Geology*, vol. 160, pp. 21–33, 2013.
[8] Y. M. Cheng, T. Lansivaara, and W. B. Wei, "Two-dimensional slope stability analysis by limit equilibrium and strength reduction methods," *Computers and Geotechnics*, vol. 34, no. 3, pp. 137–150, 2007.
[9] Z. H. Dai and P. S. Shen, "Numerical solution of simplified Bishop method for stability analysis of soil slopes," *Rock and Soil Mechanics*, vol. 23, no. 6, pp. 760–764, 2002.
[10] A. J. Li, R. Merifield, and A. V. Lyamin, "Limit analysis solutions for three dimensional undrained slopes," *Computers and Geotechnics*, vol. 36, no. 8, pp. 1330–1351, 2009.
[11] H. Z. Li, B. Bin, X. L. Chen, Y. Yao, and Y. J. Mao, "Stability analysis on the gently-inclined stepped slope with weak interlayer under hydraulic action," *Mining Research and Development*, vol. 37, no. 11, pp. 41–45, 2017.
[12] J. Jin, H. Zhang, L. Xu, K. Zhou, and X. Lv, "Stability analysis of downstream dam expansion tailings pond," *Advances in Civil Engineering*, vol. 2022, Article ID 1809736, 13 pages, 2022.
[13] G. Fan, J. J. Zhang, and X. Fu, "Reasearch on transfer function of bedding rock slope with soft interlayers and its application," *Rock and Soil Mechanics*, vol. 38, no. 4, pp. 1052–1059, 2017.
[14] J. Li, B. Zhang, and B. Sui, "Stability analysis of rock slope with multilayer weak interlayer," *Advances in Civil Engineering*, vol. 2021, Article ID 1409240, 9 pages, 2021.
[15] Q. Cai, W. Zhou, J. Shu, Y. Liu, and H. Peng, "Analysis and opplicaiton on end-slope timeliness of internal dumping under flat dipping ore body in large surface coal mine," *Journal of China University of Mining & Technology*, vol. 37, no. 6, pp. 740–744, 2008.
[16] L. Wang, D. Sun, B. Chen, and J. Li, "Three-dimensional seismic stability of unsaturated soil slopes using a semi-analytical method," *Computers and Geotechnics*, vol. 110, pp. 296–307, 2019.
[17] B. S. Firincioglu and M. Ercanoglu, "Insights and perspectives into the limit equilibrium method from 2D and 3D analyses," *Engineering Geology*, vol. 281, Article ID 105968, 2021.
[18] R. K. H. Ching and D. G. Fredlund, "Some difficulties associated with the limit equilibrium method of slices," *Canadian Geotechnical Journal*, vol. 20, no. 4, pp. 661–672, 1983.
[19] X. An, N. Li, P. Zhang, and W. Sun, "Error source analysis and precision assessment of limit equilibrium methods for rock slopes," *Advances in Civil Engineering*, vol. 2018, Article ID 3280734, 13 pages, 2018.
[20] S. Shu, B. Ge, Y. Wu, and F. Zhang, "Probabilistic assessment on 3D stability and failure mechanism of undrained slopes based on the kinematic approach of limit analysis," *International Journal of Geomechanics*, vol. 23, no. 1, Article ID 06022037, 2023.
[21] F. Pastor and E. Loute, "Limit analysis decomposition and finite element mixed method," *Journal of Computational and Applied Mathematics*, vol. 234, no. 7, pp. 2213–2221, 2010.
[22] C. Sun, J. Chai, Z. Xu, Y. Qin, and X. Chen, "Stability charts for rock mass slopes based on the Hoek-Brown strength reduction technique," *Engineering Geology*, vol. 214, pp. 94–106, 2016.
[23] S. Xiao, H. Liu, and X. Yu, "Analysis method of seismic overall stability of soil slopes retained by gravity walls anchored horizontally with flexible reinforcements," *Rock and Soil Mechanics*, vol. 41, no. 6, pp. 1836–1844, 2020.
[24] R. L. Michalowski, "Slope stability analysis: a kinematical approach," *Géotechnique*, vol. 45, no. 2, pp. 283–293, 1995.
[25] I. B. Donald and Z. Chen, "Slope stability analysis by the upper bound approach: fundamentals and methods," *Canadian Geotechnical Journal*, vol. 34, no. 6, pp. 853–862, 1997.
[26] Z. H. Bo, X. U. Baotian, Y. A. Changhong, and W. A. Wei, "Numerical analysis of slope stability for artificial land-scape hill," *Journal of Engineering Geology*, vol. 19, no. 6, pp. 859–864, 2011.
[27] Z. Q. Huang, L. F. Wu, A. M. Wang, and T. Jiang, "Stability analysis of expansive soil slope based on in-situ shear test," *Rock and Soil Mechanics*, vol. 7, pp. 1764–1768, 2008.
[28] B. Sun and Q. Liang, "Back analysis of general slope under earthquake forces using upper bound theorem," *Journal of Central South University*, vol. 20, no. 11, pp. 3274–3281, 2013.
[29] Y. F. Gao, F. Zhang, G. H. Lei, and D. Y. Li, "An extended limit analysis of three-dimensional slope stability," *Géotechnique*, vol. 63, no. 6, pp. 518–524, 2013.

[30] H. Lin and J. Y. Chen, "Back analysis method of homogeneous slope at critical state," *KSCE Journal of Civil Engineering*, vol. 21, no. 3, pp. 670–675, 2017.

[31] G. Fan, L. M. Zhang, J. J. Zhang, and C. W. Yang, "Time-frequency analysis of instantaneous seismic safety of bedding rock slopes," *Soil Dynamics and Earthquake Engineering*, vol. 94, pp. 92–101, 2017.

[32] J. Chen, J. H. Yin, and C. F. Lee, "Upper bound limit analysis of slope stability using rigid finite elements and nonlinear programming," *Canadian Geotechnical Journal*, vol. 40, no. 4, pp. 742–752, 2003.

[33] Y. Q. Liu, H. B. Li, K. Q. Xiao, J. C. Li, X. Xia, and B. Liu, "Seismic stability analysis of a layered rock slope," *Computers and Geotechnics*, vol. 55, pp. 474–481, 2014.

[34] T. K. Nian, G. Q. Chen, M. T. Luan, Q. Yang, and D. F. Zheng, "Limit analysis of the stability of slopes reinforced with piles against landslide in nonhomogeneous and anisotropic soils," *Canadian Geotechnical Journal*, vol. 45, no. 8, pp. 1092–1103, 2008.

[35] Z. Wang, X. Yang, and A. Li, "Upper bound limit stability analysis for soil slope with nonuniform multiparameter distribution based on discrete algorithm," *Advances in Civil Engineering*, vol. 2020, Article ID 7452656, 9 pages, 2020.

[36] G. P. Tang, L. H. Zhao, L. Li, and J. Y. Chen, "Combined influence of nonlinearity and dilation on slope stability evaluated by upper-bound limit analysis," *Journal of Central South University*, vol. 24, no. 7, pp. 1602–1611, 2017.

[37] T. Shogaki and N. Kumagai, "A slope stability analysis considering undrained strength anisotropy of natural clay deposits," *Soils and Foundations*, vol. 48, no. 6, pp. 805–819, 2008.

[38] Z. G. Qian, A. J. Li, A. V. Lyamin, and C. C. Wang, "Parametric studies of disturbed rock slope stability based on finite element limit analysis methods," *Computers and Geotechnics*, vol. 81, pp. 155–166, 2017.

[39] C. W. W. Ng and Y. W. Pang, "Influence of stress state on soilwater characteristics and slope stability," *Journal of Geotechnical and Geoenvironmental Engineering*, vol. 126, no. 2, pp. 157–166, 2000.

[40] J. Xiao, H. Yang, J. Zhang, and X. Tang, "Properties of drained shear strength of expansive soil considering low stresses and its influencing factors," *International Journal of Civil Engineering*, vol. 16, no. 10, pp. 1389–1398, 2018.

[41] Y. M. Cheng, D. Z. Li, L. Li, Y. J. Sun, R. Baker, and Y. Yang, "Limit equilibrium method based on an approximate lower bound method with a variable factor of safety that can consider residual strength," *Computers and Geotechnics*, vol. 38, no. 5, pp. 623–637, 2011.

[42] X. Jiang, J. Niu, H. Yang, and F. Wang, "Upper bound limit analysis for seismic stability of rock slope with tunnel," *Advances in Civil Engineering*, vol. 2018, Article ID 3862974, 11 pages, 2018.